AIAA JOURNAL
Vol. 44, No. 9, September 2006

Effects of Bridging on Buckling of Trilayer Beams with Separated Delaminations

M. Parlapalli* and D. Shu†
Nanyang Technological University, Singapore, 639798, Republic of Singapore

DOI: 10.2514/1.20248

Effective-bridging modulus, a new nondimensionalized parameter, is defined and introduced in the present work to study the influence of bridging on the delamination buckling of a trilayer beam with two separated delaminations. A generalized mathematical model is developed by using the Rayleigh–Ritz energy method and is solved as an eigenvalue problem. The reinforcement of stitching threads is assumed to provide continuous linear restoring tractions opposing the opening of the delaminations. Because of the presence of the two separated delaminations, the trilayer beam is analyzed as seven interconnected beams using the delaminations as their boundaries. Lagrange multipliers are used to enforce the boundary and continuity conditions between the interconnected beams. Parametric studies in terms of the sizes and locations of the delaminations on the buckling load have been carried out. It is observed that bridging strongly influences the buckling load and a monotonic relation is observed between the buckling load and the effective-bridging modulus. The bridging is found to be effective for thin and shallow delaminations of moderate lengths. Spanwise positions of the delaminations strongly influence the buckling loads. In addition, an analytical model for obtaining the upper bounds of the buckling load is presented.

I. Introduction

DELAMINATIONS are common failure modes of the composite laminates, which arise due to the manufacturing errors (e.g., by an imperfect curing process) or in-service accidents (e.g., low velocity impacts). Under compressive loads, a delaminated composite laminate may buckle and possibly undergo propagation of the delaminations. This in turn can lead to lowering of the buckling load of the laminate and lead to an unexpected structural failure at loads below the design level. It has been demonstrated experimentally and theoretically that adequate through-thickness reinforcement prevents the unstable growth of the delaminations by bridging the delamination cracks [1]. Several authors have investigated the buckling behavior of the delaminated composite beams, plates, and shells without considering the bridging [2–11]. The through-thickness reinforcements include stitching or weaving continuous fiber tows and inserting discontinuous fibrous or metal rods [12]. Some researchers have focused on the material improvements to increase the resistance to delamination, that is, on the use of tougher matrices or better fiber/matrix interface or interleaving concepts [13,14]. The biggest advantage of the stitching when compared with other methods of the through-thickness reinforcement is its versatility. Bridging and stitching between the delaminated laminae work together to delay both the delamination buckling and further delamination expansion and therefore have a favorable effect on the load bearing capability under edgewise compression [15]. Stitched composites have been shown in many cases to have considerable promise for some load bearing structures. In the aerospace industry stitched composites have been used in the new generation primary structures for commercial aircraft such as fuselages and wings. In addition, stitched composites are being assessed for use in automotive components such as bumper bars, floor panels, and door members. These applications are showing encouraging signs for the widespread use of stitched composites in marine, land transport, and civil infrastructures. In all of the above cases, an optimum level of stitching should be sought for the structure to withstand maximum loads.

Shu and Mai [16,17] showed that adequate crack bridging by stitching significantly increases the buckling strength of delaminated composites as well as delays the delamination propagation. Cox [18] observed that the delamination buckling occurs only if the delamination length reaches to a particular characteristic length for thin delaminated beams with stitching. He and Cox [19] suggested that for cases of curved laminar structures, stitching is effective in suppressing the crack opening if the ratio between the laminate half-thickness and stitch radius is above five. Hu et al. [20] observed that the buckling load decreases monotonically with the increase of the circular delamination radius. Pan and Herrington [21] noted that the increase of the stitching thread diameter results in a higher local buckling strength and reduction in the in-plane strength. Li et al. [22] observed that the bridging force changes the catastrophic nature of the delamination growth and increases the stability of the delamination. Also they noted that the higher the material fracture toughness, the higher the stability of the delamination growth, and the smaller the range and dynamic effect of its unstable growth. Gui and Li [23] investigated the thin film buckling analysis of stitched composite laminates with an embedded elliptical delamination by employing the Rayleigh–Ritz energy method. They noted a significant effect of stitching on the buckling strains and buckling modes and observed multiple humps in the buckling configurations for cases of larger delamination sizes. Daridon and Zidani [24] investigated the influence of fiber bridging at a crack tip on the propagation due to the local buckling of an existing crack in composite plates under a compressive load. Recently more investigation has been focused on the crack bridging by metallic rods [25] and z fibers [26]. Short rods have been advocated as a cost-effective method of increasing the delamination resistance [27].

The effects of bridging on the delamination buckling of trilayer beams with two separated delaminations have not yet been studied. Recently, the present authors studied the effects of bridging on the delamination buckling of a two-layer delaminated beam by introducing a nondimensionalized parameter, effective-bridging modulus [28]. In the present work, a generalized mathematical model is developed to study the effects of bridging on the delamination buckling of trilayer beams with two separated delaminations by using the Rayleigh–Ritz energy method, which is solved as an eigenvalue problem. Further, upper bounds of the buckling load are obtained by developing a mathematical model based on the

Received 25 September 2005; revision received 8 March 2006; accepted for publication 12 May 2006.

*Postdoctoral Research Associate, School of Mechanical and Aerospace Engineering; madhu@ntu.edu.sg.

†Associate Professor, School of Mechanical and Aerospace Engineering, N2-01b-44, 50 Nanyang Avenue; mdshu@ntu.edu.sg.

Euler–Bernoulli beam theory and by incorporating the appropriate kinematic continuity and boundary conditions. Results are compared with the literature for a homogeneous delaminated beam case. Parametric studies in terms of the sizes and locations of the delaminations on the buckling load are carried out for homogenous and trilayer delaminated beams. The values of the effective-bridging modulus (BM) are chosen for the range of values expected for trilayer beams made of different material layer combinations. A case study involving the bridging effects on the delamination buckling analysis of a trilayer beam made of carbon/epoxy, glass/epoxy, and carbon/epoxy layers with two separated delaminations has been presented. A similar analysis can be carried out for different trilayer beams, made of different materials such as glass/epoxy, carbon/epoxy, and glass/epoxy, etc. From these studies an optimum level of stitching can be sought to maximize the strength of the trilayer delaminated beam.

The following section deals with the mathematical modeling of the present problem. Initially, formulations for lower and upper bounds of the buckling load are presented based on the Euler–Bernoulli beam theory. Later, the formulation of a generalized mathematical model based on the energy method is presented. Finally, the results are presented.

II. Formulation

A. Problem Definition

The geometry of a trilayer bridged beam with two separated delaminations is shown in Fig. 1a. The beam is made of three distinctive material layers (layers 2, 8, and 6), with thicknesses H_2, H_8, and H_6, Young's moduli E_2, E_8, and E_6 and Poisson ratios ν_2, ν_8, and ν_6, respectively. The length of the beam is L and thickness is H. The two preexisting separated through the width delaminations are denoted as delamination I (of length a, lying between layers 2 and 8 and located at an offset distance of d_1 from the center of the beam) and delamination II (of length b, lying between layers 8 and 6 and located at an offset distance of d_2 from the center of the beam). Since the delaminations are asymmetrically located, the whole beam configuration is considered while developing the mathematical models. Considering the through the width delaminations conveniently defines the unit width of the trilayer beam. Both ends of the beam are assumed to be clamped and an external load P is applied along the neutral axis of the beam. Because of the presence of the two separated delaminations, the trilayer beam is analyzed as seven interconnected beams, that is, virgin beams 1, 4, and 7 (nondelaminated region), and subbeams 2, 3, 5, and 6 (delaminated region) as shown in Figs. 1b and 2. In Fig. 2, the equivalent beam model is shown with the neutral axes of the virgin and subbeams. The virgin and subbeams have thicknesses of H_i and lengths of L_i ($i = 1$–7), respectively. In Fig. 1a, points A and F denote the clamped ends and B, C, D, and E denote the delamination ends. The delaminated beam is assumed to be reinforced in the through-thickness direction by stitches having a bridging modulus of K as shown in Fig. 3a and the corresponding beam under compressive loading is shown in Fig. 3b. The bridging modulus depends on the density and stiffness of the stitches. The coordinate axes for the subbeams are shown in Fig. 3b, and x is measured from the left end of the trilayer beam, $W_i(x)$ denotes the small elastic deflection of the

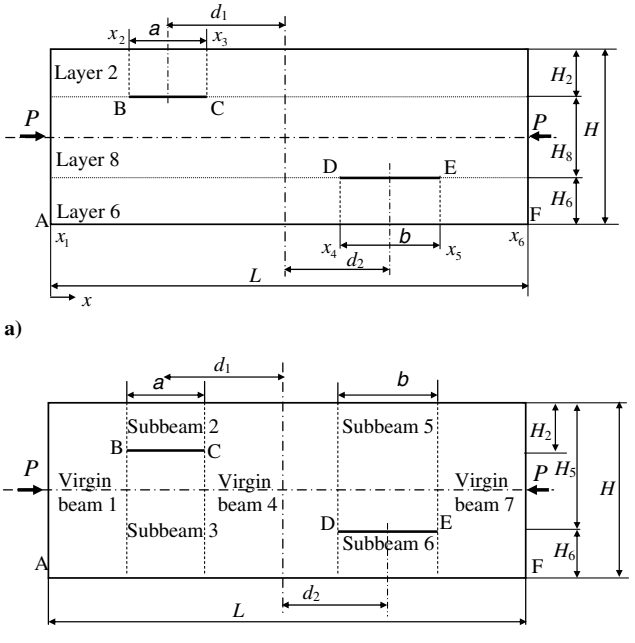

Fig. 1 a) A trilayer beam with two separated delaminations; b) an equivalent beam model of the trilayer beam with two separated delaminations.

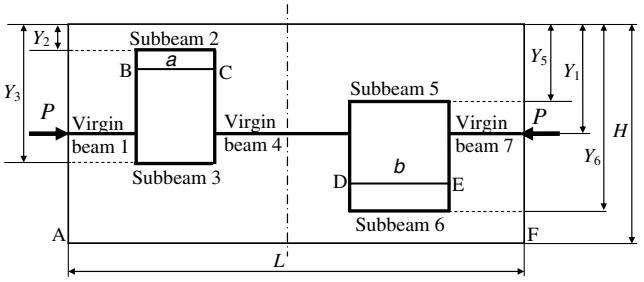

Fig. 2 Equivalent beam model shown with neutral axes positions.

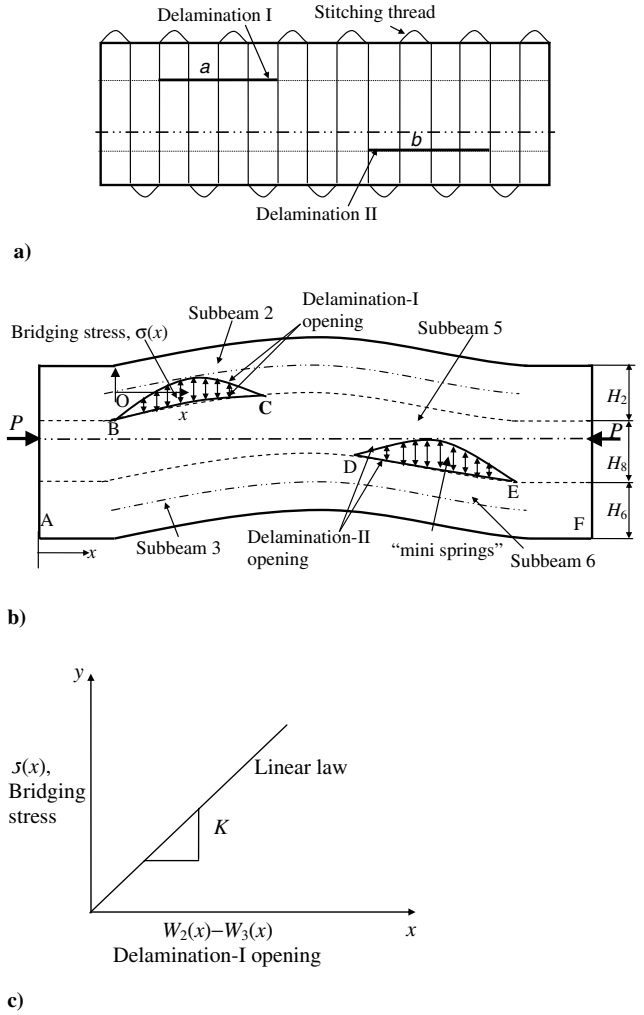

Fig. 3 a) Trilayer delaminated beam with bridging; b) trilayer delaminated beam with bridging under compressive loading (shown with openings of the two separated delaminations); c) linear bridging model.

neutral axis of the virgin and subbeams ($i = 1$–7). If the spacing of the stitching threads is appreciably smaller than the delamination lengths, the reinforcement of the stitching threads is assumed to provide continuous restoring tractions opposing the deflection of the delaminated layers. So, the stitching stress $\sigma(x)$ and the delamination opening $\Delta W(x)$ (for the case of delamination I, the difference between the deflections of the two subbeams 2 and 3, that is, $W_2(x)$ and $W_3(x)$; for the case of delamination II, the difference between the deflections of the two subbeams 5 and 6, that is, $W_5(x)$ and $W_6(x)$) are assumed to be related by the Winkler elastic foundation model, that is, $\sigma(x) = K\Delta W(x)$, as shown in Fig. 3c. The Winkler elastic foundation type of law has been successfully implemented previously by various researchers for studying the delamination buckling with bridging [17,18,20,23]. When $K \to \infty$, the upper bounds of the buckling load of a trilayer beam with two separated delaminations will be obtained. If the spring constant approaches zero ($K \to 0$), it can be modeled as a nonbridging delamination problem and that gives the lower bounds of the buckling load [17]. A direct measurement of K is difficult and it can be obtained by conducting experiments on two double cantilever specimens with and without stitching. The difference in compliance between the stitched and unstitched specimens then may be used to calculate the bridging modulus. K can also be computed from the elastic modulus and density of the stitches. If the laminated composite is stitched after curing of the composite, little bonding exists between the stitches and the matrix so that K can be readily calculated. If the composite laminate is stitched before curing, complicated analyses involving fiber debonding and/or pullout may have to be employed [17]. To simplify the analysis it is assumed that each layer of the beam is homogeneous and linearly elastic in nature. The compressive load is uniform and uniaxial, and the delaminations exist before the application of the load.

B. Basic Equations

For virgin beams 1, 4, and 7, the equilibrium equation of moment is given by

$$(EI)_i W_i''(x) + P_i W_i(x) + Q_{i0}x + M_{i0} = 0 \qquad (i = 1, 4, 7) \quad (1a)$$

where $(EI)_i$ is the flexural rigidity, $W_i''(x) = d^2W_i(x)/dx^2$, P_i is the axial load ($P = P_1 = P_4 = P_7$), Q_{i0} and M_{i0} are the shear force and bending moment at the delamination ends. The flexural rigidities are given by

$$(EI)_1 = (EI)_4 = (EI)_7 = (EI)_2 + (EI)_8 + (EI)_6 + \bar{E}_2H_2(Y_1 - Y_2)^2 + \bar{E}_8H_8(Y_1 - Y_8)^2 + \bar{E}_6H_6(Y_1 - Y_6)^2$$

where Y_i ($i = 1, 2, 6, 8$) are the neutral axis positions of the ith beam which are given by $Y_1 = (\bar{E}_2H_2Y_2 + \bar{E}_8H_8Y_8 + \bar{E}_6H_6Y_6)/(\bar{E}_2H_2 + \bar{E}_8H_8 + \bar{E}_6H_6)$, $Y_8 = H_2 + H_8/2$, $Y_2 = H_2/2$, $Y_3 = (\bar{E}_8H_8Y_8 + \bar{E}_6H_6Y_6)/(\bar{E}_8H_8 + \bar{E}_6H_6)$, $Y_5 = (\bar{E}_8H_8Y_8 + \bar{E}_2H_2Y_2)/(\bar{E}_8H_8 + \bar{E}_2H_2)$ and $Y_6 = H_2 + H_8 + H_6/2$. The flexural rigidities of subbeams 2, 6, and 8 are given by $(EI)_2 = \bar{E}_2H_2^3/[12(1 - \upsilon_2^2)]$, $(EI)_6 = \bar{E}_6H_6^3/[12(1 - \upsilon_6^2)]$, and $(EI)_8 = \bar{E}_8H_8^3/[12(1 - \upsilon_8^2)]$, for isotropic materials and $(EI)_2 = (\bar{E}_2)_{11}H_2^3/[12(1 - \upsilon_{12}\upsilon_{21})_2]$, $(EI)_6 = (\bar{E}_6)_{11}H_6^3/[12(1 - \upsilon_{12}\upsilon_{21})_6]$, and $(EI)_8 = (\bar{E}_8)_{11}H_8^3/[12(1 - \upsilon_{12}\upsilon_{21})_8]$, for orthotropic materials, where $\bar{E}_j = E_j$ stands for plane stress and $\bar{E}_j = E_j/(1 - \upsilon_j^2)$ stands for plane strain problems [29]. The subscript 11 represents the fiber direction. Subbeams 3 and 5 are bimaterial beams made up of materials having Young's moduli E_6 and E_8, E_2 and E_8, respectively. The flexural rigidities of subbeams 3 and 5 are given by $(EI)_3 = (EI)_8 + (EI)_6 + (\bar{E}H)_8(Y_3 - Y_8)^2 + (\bar{E}H)_6(Y_3 - Y_6)^2$ and $(EI)_5 = (EI)_2 + (EI)_8 + (\bar{E}H)_8(Y_5 - Y_8)^2 + (\bar{E}H)_2(Y_5 - Y_2)^2$, respectively.

By differentiating Eq. (1a) twice, the Q_{i0} and M_{i0} terms will be eliminated. Therefore, Eq. (1a) is differentiated twice to yield the differential equation governing the buckling of the virgin beams 1, 4, and 7 as

$$(EI)_{ii}''''(x) + P_i W_i''(x) = 0 \qquad (i = 1, 4, 7) \qquad (1b)$$

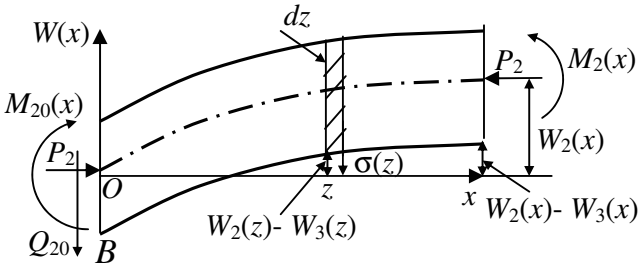

Fig. 4 Moment equilibrium for subbeam 2.

For subbeam 2, the moment equilibrium of segment Ox about x yields (by integrating a small strip of length dz from O to x, Figs. 3b and 4)

$$(EI)_2W_2''(x) + P_2W_2(x) + \int_{x_2}^{x} K[W_2(z) - W_3(z)](x - z)\mathrm{d}z + Q_{20}x + M_{20} = 0 \qquad (2)$$

Differentiating Eq. (2) twice gives the following fourth-order differential equation:

$$(EI)_2W_2''''(x) + P_2W_2''(x) + K[W_2(x) - W_3(x)] = 0 \qquad (3)$$

Similarly to that of subbeam 2, the equation governing the buckling of subbeam 3 is given by

$$(EI)_3W_3''''(x) + P_3W_3''(x) + K[W_3(x) - W_2(x)] = 0 \qquad (4)$$

Similarly, for subbeam 5, the equation governing the buckling is given by

$$(EI)_5W_5''''(x) + P_5W_5''(x) + K[W_5(x) - W_6(x)] = 0 \qquad (5)$$

Similarly, for subbeam 6, the equation governing the buckling is given by

$$(EI)_6W_6''''(x) + P_6W_6''(x) + K[W_6(x) - W_5(x)] = 0 \qquad (6)$$

III. Mathematical Model: Lower Bounds of the Critical Buckling Load

The lower bounds of the critical buckling load of a trilayer bridged beam with two separated delaminations are obtained by neglecting the bridging stresses, that is, $\sigma(x) = 0$, which leads to $K = 0$. This problem degenerates into a nonbridging delamination and this case has been recently studied by the current authors [30] and those results are quoted here as the lower bounds of the buckling load.

IV. Mathematical Model: Upper Bounds of the Critical Buckling Load

In this section a mathematical model will be developed based on the Euler–Bernoulli beam theory and by incorporating appropriate kinematic continuity and boundary conditions to obtain the upper bounds of the buckling load of a trilayer delaminated with two separated delaminations. The developed mathematical model will be solved as an eigenvalue problem. The upper bounds are obtained by an infinitely strong through-thickness reinforcement which means $K \to \infty$. Intuitively, stronger bridging (i.e., large K) yields a stronger structure and thus a higher buckling load. When $K \to \infty$, subbeams 2 and 3 have the same flexural deformation [17] which gives rise to $W_2(x) = W_3(x)$. Hence, for subbeam 2, Eq. (3) is simplified as

$$(EI)_2W_2''''(x) + P_2W_2''(x) = 0 \qquad (7)$$

Similarly, for subbeam 3, Eq. (4) changes into

$$(EI)_3W_2''''(x) + P_3W_2''(x) = 0 \qquad (8)$$

Thus, from Eqs. (7) and (8), the following relation is obtained:

$$\frac{P_2}{(EI)_2}=\frac{P_3}{(EI)_3}=\frac{P_2+P_3}{(EI)_2+(EI)_3}=\frac{P}{(EI)_2+(EI)_3} \tag{9}$$

The general solution of Eqs. (7) and (8) is given by

$$W_2(x)=W_3(x)=A_2\cos(\lambda_2 x)+B_2\sin(\lambda_2 x)+C_2x+D_2 \tag{10}$$

where A_2, B_2, C_2, and D_2 are integration coefficients and $\lambda_2=\sqrt{P_2/(EI)_2}$.

Similarly, subbeams 5 and 6 have the same flexural deformations when $K\to\infty$, which give rise to $W_5(x)=W_6(x)$. Hence, for subbeam 5, Eq. (5) is simplified as

$$(EI)_5W_5''''(x)+P_5W_5''(x)=0 \tag{11}$$

Similarly, for subbeam 6, Eq. (6) changes into

$$(EI)_6W_5''''(x)+P_6W_5''(x)=0 \tag{12}$$

Thus, from Eqs. (11) and (12), the following relation is obtained:

$$\frac{P_5}{(EI)_5}=\frac{P_6}{(EI)_6}=\frac{P_5+P_6}{(EI)_5+(EI)_6}=\frac{P}{(EI)_5+(EI)_6} \tag{13}$$

The general solution of Eqs. (11) and (12) is given by

$$W_5(x)=W_6(x)=A_5\cos(\lambda_5 x)+B_5\sin(\lambda_5 x)+C_5x+D_5 \tag{14}$$

where A_5, B_5, C_5, and D_5 are integration coefficients and $\lambda_5=\sqrt{P_5/(EI)_5}$.

For virgin beams 1, 4, and 7, the governing equation is given by Eq. (1b) which has general solutions of the form:

$$W_i(x)=A_i\cos(\lambda_i x)+B_i\sin(\lambda_i x)+C_ix+D_i \qquad (i=1,4,7) \tag{15}$$

where A_i, B_i, C_i, and D_i ($i=1$, 4, and 7) are integrations coefficients and $\lambda_i=\sqrt{P_i/(EI)_i}$ ($i=1$, 4, 7). From the general solutions of the virgin and subbeams [Eqs. (10), (14), and (15)], there exists 20 unknown variables (A_i, B_i, C_i, and D_i; $i=1$, 2, 4, 5, and 7) and it requires 20 equations to solve for these variables in order to solve it as an eigenvalue problem. These 20 equations will be obtained from the boundary and continuity conditions, which are discussed next.

A. Basic Equations

1. Boundary Conditions

For clamped ends at $x=x_1$:

$$W_1(x_1)=0 \tag{16}$$

and

$$W_1'(x_1)=0 \tag{17}$$

at $x=x_6$:

$$W_7(x_6)=0 \tag{18}$$

and

$$W_7'(x_6)=0 \tag{19}$$

Continuity conditions at $x=x_2=L/2-a/2+d_1$ between the virgin beam 1 and subbeams 2 and 3:

displacement continuity:

$$W_1(x_2)=W_2(x_2) \tag{20}$$

slope continuity:

$$W_1'(x_2)=W_2'(x_2) \tag{21}$$

shear force continuity:

$$Q_1(x=x_2)=Q_{20}+Q_{30} \tag{22}$$

bending moment continuity:

$$M_1(x=x_2)=M_{20}+M_{30}-\Delta P_2(|Y_1-Y_2|)+\Delta P_3(|Y_1-Y_3|) \tag{23}$$

where $M_i(x)=-(EI)_iW_i''(x)$, $Q_i(x)=-(EI)_iW_i'''(x)$, ΔP_2 and ΔP_3 are the incremental axial forces in subbeams 2 and 3, arising from the axial extension/compression. Before buckling occurs, the axial strains in subbeams 2 and 3 are identical. When buckling takes place, the axial stress in the buckled subbeam decreases and varies. This induces changes in the axial forces in subbeams 2 and 3, which are denoted as ΔP_2 and ΔP_3. In the same process, similar continuity conditions can be obtained at $x=x_3$ between the virgin beam 4 and subbeams 2 and 3.

Continuity conditions at $x=x_4=L/2-b/2+d_2$ between the virgin beam 4 and subbeams 5 and 6:

displacement continuity:

$$W_4(x_4)=W_5(x_4) \tag{24}$$

slope continuity:

$$W_4'(x_4)=W_5'(x_4) \tag{25}$$

shear force continuity:

$$Q_4(x=x_4)=Q_{50}+Q_{60} \tag{26}$$

bending moment continuity:

$$M_4(x=x_4)=M_{50}+M_{60}-\Delta P_5(|Y_4-Y_5|)+\Delta P_6(|Y_4-Y_6|) \tag{27}$$

where ΔP_5 and ΔP_6 are the incremental axial forces in subbeams 5 and 6, arising from the axial extension/compression. In the same process, similar continuity conditions can be obtained at $x=x_5$ between virgin beam 7 and subbeams 5 and 6.

2. Additional Conditions

Because of the moment continuity conditions as Eqs. (23) and (27), there are four additional unknown variables in the form of ΔP_2, ΔP_3, ΔP_5, and ΔP_6. Hence the number of unknowns increases to 24 (A_i, B_i, C_i, and D_i, $i=1$, 2, 4, 5, and 7; and ΔP_2, ΔP_3, ΔP_5, and ΔP_6), and it requires one to have four additional conditions to solve for all these variables.

The axial force balance at $x=x_2$:

$$\Delta P_2+\Delta P_3=0 \tag{28}$$

The axial force balance at $x=x_3$

$$\Delta P_6+\Delta P_5=0 \tag{29}$$

Based on the axial equilibrium of the stretching/shortening of subbeam 3, we have [30]

$$L_3^0=L_3+|Y_1-Y_3|(\theta_2-\theta_1) \tag{30}$$

Similarly, for subbeam 5 [30]:

$$L_5^0=L_5+|Y_5-Y_1|(\theta_4-\theta_3) \tag{31}$$

where L_3^0 and L_5^0 are the length of the beam after stretching/shortening; $L_3=a$; $L_5=b$; θ_1, θ_2, θ_3, θ_4 are the slopes at the delamination fronts x_2, x_3, x_4, and x_5, respectively which are given by

$$\begin{aligned}&\theta_1=W_1'(x=x_2), \qquad \theta_2=W_2'(x=x_3),\\ &\theta_3=W_4'(x=x_4), \quad \text{and} \quad \theta_4=W_5'(x=x_5)\end{aligned} \tag{32}$$

B. Nondimensionalization

Nondimensionalization is a process of converting parameters with units to parameters without units, which starts with a choice of the scales for the problem. It is essential and important to note that the boundary conditions also have to be nondimensionalized besides the various continuity conditions. The lengths of delaminations I and II (a and b), the locations of the delaminations along the spanwise positions (d_1 and d_2), neutral axial positions (Y_i), individual beam thicknesses (H_i) are nondimensionalized as $\bar{a} = a/L$, $\bar{b} = b/L$, $\bar{d}_1 = d_1/L$, $\bar{d}_2 = d_2/L$, $\bar{H}_i = H_i/H$, and $\bar{Y}_i = Y_i/$ $(i - 1–8)$.

The buckling load is nondimensionalized as $\bar{P} = P/P_{\text{cr}}$, where for clamped supports, the critical buckling load is given by $P_{\text{cr}} = 4\pi^2(EI)_1/L^2$. Other parameters are nondimensionalized as $\bar{\lambda}_1 = \lambda_1 L = 2\pi\sqrt{\bar{P}_1} = \bar{\lambda}_4 = \bar{\lambda}_7$; $\bar{\lambda}_i = \lambda_i L = \sqrt{P_i L^2/(EI)_i}$ $(i = 2, 3, 5, 6)$. The 20 integration coefficients have been nondimensionalized as $\bar{A}_i = A_i/H$; $\bar{B}_i = B_i/H$; $\bar{C}_i = C_i L/H$; $\bar{D}_i = D_i/H$ $(i = 1, 2, 4, 5, 7)$. The incremental forces are nondimensionalized as $\Delta\bar{P}_i = \Delta P_i/P_{\text{cr}}$ $(i = 1, 2, 3, 5, 6)$.

C. Eigenvalue Problem

The above 16 equations [Eqs. (16–31)] and eight continuity conditions at the delamination fronts $x = x_3$ and $x = x_5$ are nondimensionalized and the coefficients of the 20 four unknown variables are written in a matrix form. Because of the nondimensionalization of the above equations, the nondimensionalized buckling load ($\bar{P} = P/P_{\text{cr}}$) depends on the material and geometrical parameters (lengths and locations of the two separated delaminations, trilayer beam material properties, and beam configurations). For a nontrivial solution to exist the determinant of the coefficient matrix must vanish and the lowest eigenvalue gives the critical buckling load. The system of homogeneous equations which governs buckling of the delaminated beam are nondimensionalized and are written in the form of a matrix as

$$[P]\{A\} = 0 \tag{33}$$

where $[P]$ is a 24×24 matrix and

$$\{A\}^T = \{\bar{A}_1, \bar{B}_1, \bar{C}_1, \bar{D}_1, \bar{A}_2, \bar{B}_2, \bar{C}_2, \bar{D}_2, \bar{A}_4, \bar{B}_4, \bar{C}_4, \bar{D}_4, \bar{A}_5, \bar{B}_5, \bar{C}_5, \bar{D}_5, \bar{A}_7, \bar{B}_7, \bar{C}_7, \bar{D}_7, \Delta\bar{P}_2, \Delta\bar{P}_3, \Delta\bar{P}_5, \Delta\bar{P}_6\}$$

The characteristic equation is given by

$$|P_{ij}| = 0 \qquad (i, j = 1–24) \tag{34}$$

and the lowest eigenvalue ($\bar{\lambda}$) is a measure of the buckling load. The LDU decomposition method [31] (any square matrix can be written as the product of a lower triangular, an upper triangular, and a diagonal matrix. This product is called an LDU decomposition of the matrix) and root bisection methods have been used to find out the roots of the characteristic equation, Eq. (34). FORTRAN programs based on the above theory have been developed and the values are computed for different case studies, which are presented in the results section.

V. Mathematical Model-Delamination Buckling Loads with Bridging by an Energy Method

The lower and upper bounds of the buckling load are obtained in the earlier sections by means of analytical methods. The lower bounds of the buckling load are obtained when $K = 0$ (no bridging) whereas the upper bounds of the buckling load are obtained when $K \to \infty$ (infinitely strong bridging). To study the effects of bridging on the delamination buckling, a mathematical model will be developed in this section by using the Rayleigh–Ritz energy method as the present problem becomes nonlinear due to the presence of bridging. Energy methods have been successfully used to obtain approximate buckling loads of delaminated beams by various researchers [21,23,32]. The successful application of the Rayleigh–Ritz method hinges largely on the appropriate choice of the coordinate functions. In general, each term of the expansion should satisfy the geometric boundary conditions and kinematic constraints associated with the problem, which limits the choice of functions in many case. However, if Lagrange multipliers are included in the energy expression, each term of the expansion need not satisfy the geometric boundary conditions or constraints [32]. The potential energy of the trilayer bridged beam with two separated delaminations is denoted by $\tilde{\Pi}$ which is written as

$$\tilde{\Pi} = \Pi(a_1, a_2, \ldots, a_n) - \alpha_1 f_1 - \alpha_2 f_2 - \cdots - \alpha_r f_r \tag{35}$$

where Π is the initial potential energy of the system when there are no Lagrange multipliers present; $a_1, a_2, \ldots, a_n$ are several coordinate functions, representing the displacement function, α_r are the Lagrange multipliers, and the r equations are given by

$$f_r(a_1, a_2, \ldots, a_n) = 0 \tag{36}$$

Equation (35) contains a group of equations, obtained from the kinematic constraint conditions which include both the geometric boundary and kinematic continuity conditions that must be enforced between the beam regions using Lagrange multipliers in the energy method. For example, appropriate boundary conditions at the right end of the beam (i.e., $x = x_6$) are given by Eqs. (16) and (17). Constraints must be enforced at the junction of subbeams 2 and 3 and the virgin beam 1 (at $x = x_2$) to ensure that the plane sections of the beam remain plane. Similarly constraints (continuity conditions) must be enforced at the junction of subbeams 2 and 3 and the virgin beam 4 (at $x = x_3$); at the junction of subbeams 5 and 6 and the virgin beam 4 (at $x = x_4$), and at the junction of subbeams 5 and 6 and the virgin beam 7 (at $x = x_5$). In Sec. IV continuity conditions between the virgin and subbeams at the delamination fronts are presented for the case of upper bounds of the buckling loads. Similarly, continuity conditions between the virgin and subbeams at the delamination fronts can be obtained for the present case where subbeams 2 and 3 and subbeams 5 and 6 have different flexural deformations [30]. The details are omitted here. The boundary conditions for clamped conditions are given by Eqs. (16–19). Because of the Lagrange multipliers, the total number of the unknowns becomes $n + r$, which are then determined by solving the $n + r$ equations. The n number of equations are given by

$$\frac{\partial\tilde{\Pi}}{\partial a_i} = 0, \quad \text{for all } i = 1, 2, \ldots, n \tag{37}$$

and the r equations are obtained from

$$\frac{\partial\tilde{\Pi}}{\partial \alpha_i} = 0, \quad \text{for all } i = 1, 2, \ldots, r \tag{38}$$

This process leads to an eigenvalue problem, in which the lowest eigenvalue gives the nondimensionalized buckling load.

A. Basic Equations

The initial potential energy of the trilayer bridged beam with two separated delaminations is written as

$$\Pi = U_a + U_b + U_c + U_s - \Omega \tag{39}$$

where U_a is the axial strain energy which is given by

$$U_a = \frac{1}{2}\int_{x_1}^{x_2} A_{11}^1\left(\frac{\partial u_1}{\partial x}\right)^2 dx + \frac{1}{2}\int_{x_2}^{x_3}\left[A_{11}^2\left(\frac{\partial u_2}{\partial x}\right)^2 + A_{11}^3\left(\frac{\partial u_3}{\partial x}\right)^2\right]dx + \frac{1}{2}\int_{x_3}^{x_4} A_{11}^4\left(\frac{\partial u_4}{\partial X}\right)^2 dx + \frac{1}{2}\int_{x_4}^{x_5}\left[A_{11}^5\left(\frac{\partial u_5}{\partial x}\right)^2 + A_{11}^6\left(\frac{\partial u_6}{\partial x}\right)^2\right]dx + \frac{1}{2}\int_{x_5}^{x_6} A_{11}^7\left(\frac{\partial u_7}{\partial X}\right)^2 dx \tag{40}$$

U_b is the bending strain energy which is given by

$$U_b = \frac{1}{2}\int_{x_1}^{x_2} D_{11}^1\left(\frac{\partial^2 W_1}{\partial x^2}\right)^2 \mathrm{d}x + \frac{1}{2}\int_{x_2}^{x_3}\left[D_{11}^2\left(\frac{\partial^2 W_2}{\partial x^2}\right)^2 + D_{11}^3\left(\frac{\partial^2 W_3}{\partial x^2}\right)^2\right]\mathrm{d}x + \frac{1}{2}\int_{x_3}^{x_4} D_{11}^4\left(\frac{\partial^2 W_4}{\partial x^2}\right)^2 \mathrm{d}x + \frac{1}{2}\int_{x_4}^{x_5}\left[D_{11}^5\left(\frac{\partial^2 W_5}{\partial x^2}\right)^2 + D_{11}^6\left(\frac{\partial^2 W_6}{\partial x^2}\right)^2\right]\mathrm{d}x + \frac{1}{2}\int_{x_5}^{x_6} D_{11}^7\left(\frac{\partial^2 W_7}{\partial x^2}\right)^2 \mathrm{d}x \tag{41}$$

U_s is the strain energy due to stitching which is given by

$$U_s = \frac{1}{2}\int_{x_2}^{x_3} K[W_2(x) - W_3(x)]^2 \mathrm{d}x + \frac{1}{2}\int_{x_4}^{x_5} K[W_5(x) - W_6(x)]^2 \mathrm{d}x \tag{42}$$

U_c is the strain energy due to coupling between bending and stretching and is given by

$$U_c = -\frac{1}{2}\int_{x_2}^{x_3}\left[B_{11}^2\left(\frac{\partial u_2}{\partial x}\right)\left(\frac{\partial^2 W_2}{\partial x^2}\right) + B_{11}^3\left(\frac{\partial u_3}{\partial x}\right)\left(\frac{\partial^2 W_3}{\partial x^2}\right)\right]\mathrm{d}x - \frac{1}{2}\int_{x_1}^{x_2} B_{11}^1\left(\frac{\partial u_1}{\partial x}\right)\left(\frac{\partial^2 W_1}{\partial x^2}\right)\mathrm{d}x - \frac{1}{2}\int_{x_4}^{x_5} B_{11}^5\left(\frac{\partial u_5}{\partial x}\right)\left(\frac{\partial^2 W_5}{\partial x^2}\right)\mathrm{d}x - \frac{1}{2}\int_{x_4}^{x_5} B_{11}^6\left(\frac{\partial u_6}{\partial x}\right)\left(\frac{\partial^2 W_6}{\partial x^2}\right)\mathrm{d}x - \frac{1}{2}\int_{x_5}^{x_6} B_{11}^7\left(\frac{\partial u_7}{\partial x}\right)\left(\frac{\partial^2 W_7}{\partial x^2}\right)\mathrm{d}x \tag{43}$$

and Ω is the potential energy of the applied load, which is given by

$$\Omega = \frac{1}{2}\int_{x_1}^{x_2} P_1\left(\frac{\partial W_1}{\partial x}\right)^2 \mathrm{d}x + \frac{1}{2}\int_{x_2}^{x_3}\left[P_2\left(\frac{\partial W_2}{\partial x}\right)^2 + P_3\left(\frac{\partial W_3}{\partial x}\right)^2\right]\mathrm{d}x + \frac{1}{2}\int_{x_3}^{x_4} P_1\left(\frac{\partial W_4}{\partial x}\right)^2 \mathrm{d}x + \frac{1}{2}\int_{x_4}^{x_5}\left[P_5\left(\frac{\partial W_5}{\partial x}\right)^2 + P_6\left(\frac{\partial W_6}{\partial x}\right)^2\right]\mathrm{d}x + \frac{1}{2}\int_{x_5}^{x_6} P_1\left(\frac{\partial W_7}{\partial x}\right)^2 \mathrm{d}x \tag{44}$$

where $A_{11}^{(i)}$, $B_{11}^{(i)}$, and $D_{11}^{(i)}$ are the stretching, coupling, and bending stiffnesses, respectively, and u_i is the axial displacement of the ith beam. If attention is restricted to an isotropic, homogeneous material then

$$A_{11}^{(i)} = (EA)_i \tag{45}$$

$$B_{11}^{(i)} = 0 \tag{46}$$

and

$$D_{11}^{(i)} = (EI)_i \tag{47}$$

where E_i is Young's modulus, A_i is the cross-sectional area, and I_i is the moment of inertia of the ith beam, respectively. The relative in-plane displacement between subbeams 2 and 3 is given by (at an arbitrary distance x) [16]

$$\int_{x_2}^{x}\left(\frac{\mathrm{d}W_2}{\mathrm{d}x}\right)^2 \mathrm{d}x - \int_{x_2}^{x}\left(\frac{\mathrm{d}W_3}{\mathrm{d}x}\right)^2 \mathrm{d}x \tag{48}$$

since Eq. (48) contains higher order terms of the slopes of subbeams 2 and 3 and thus is neglected. Similarly, the effect of bridging on the relative in-plane displacement between subbeams 5 and 6 is neglected. In Eq. (44), P_i represents the axial load carried in each region of the beam. Because prebuckling bending deformations are neglected, we have

$$P_i = \frac{(EA)_i}{(EA)_1} P_1 \qquad (i = 2, 3, 5, 6) \tag{49}$$

Furthermore, only the bending deformation is considered in Eq. (44). This is because buckling is a bending phenomenon and the axial deformation that occurs in the equilibrium state before buckling has no bearing on the evaluation of the critical buckling loads [32]. The axial strain energy due to the axial displacements is not considered in the present analysis. In the current study, the assumed displaced shapes in each of the regions of virgin beams 1, 4, and 7 and subbeams 2, 3, 5, and 6 are the same as those of the generalized solutions, considered in the earlier works of the current authors [30], which are given by

$$W_i(x) = A_i\cos(\lambda_i x) + B_i\sin(\lambda_i x) + C_i x + D_i \qquad (i = 1\text{–}7) \tag{50}$$

where $\lambda_i = \sqrt{P_i/(EI)_i}$ $(i = 1\text{–}7)$.

B. Eigenvalue Problem

Based on the energy principle, the equilibrium condition for the trilayer bridged beam with two separated delaminations is that the total potential energy should satisfy the first derivative of the potential energy with respect to the unknown geometric coordinates and the Lagrange multipliers. The above condition produces the generalized eigenvalue problem as

$$\frac{\partial\tilde{\Pi}}{\partial a_i} = 0 \tag{51}$$

where $a_i = A_i, B_i, C_i, D_i$ $(i = 1\text{–}7)$, and α_j $(j = 1\text{–}20)$.

Equation (38) is substituted into Eq. (51) and necessary differentiation and nondimensionalization are performed to obtain the system of equations, which is solved as an eigenvalue problem. The details are omitted here due to brevity. Owing to the nondimensionalization, the bridging modulus/spring stiffness is modified and is called the effective-bridging modulus, denoted by BM, which is given by

$$\mathrm{BM} = \frac{64a^3LK}{\pi^4(EI)_1} \tag{52}$$

The BM is a function of the delamination length, slenderness ratio, and relative bridging modulus, KL/E. Equation (51) becomes a group of linear equations which are functions of the effective-bridging modulus, geometric parameters (thicknesses and lengths of individual sub- and virgin beams) and the nondimensionalized critical buckling load. These linear homogeneous equations are written in the matrix form as

$$[P]\{a_i\} = 0 \tag{53}$$

where $[P]$ is a 48×48 coefficient matrix, and $\{a_i\}$ is a 48×1 matrix containing the unknown variables, which is given by

$$\{a_i\}^T = \{\bar{A}_1, \bar{B}_1, \bar{C}_1, \bar{D}_1, \bar{A}_2, \bar{B}_2, \bar{C}_2, \bar{D}_2, \bar{A}_3, \bar{B}_3, \bar{C}_3, \bar{D}_3, \bar{A}_4, \bar{B}_4, \bar{C}_4, \bar{D}_4, \bar{A}_5, \bar{B}_5, \bar{C}_5, \bar{D}_5, \bar{A}_6, \bar{B}_6, \bar{C}_6, \bar{D}_6, \bar{A}_7, \bar{B}_7, \bar{C}_7, \bar{D}_7, \alpha 1, \alpha 2, \alpha 3, \alpha 4, \alpha 5, \alpha 6, \alpha 7, \alpha 8, \alpha 9, \alpha 10, \alpha 11, \alpha 12, \alpha 13, \alpha 14, \alpha 15, \alpha 16, \alpha 17, \alpha 18, \alpha 19, \alpha 20\}$$

The characteristic equation is given by

$$|P_{ij}| = 0 \qquad (i, j = 1\text{–}48) \tag{54}$$

and the lowest eigenvalue $(\bar{\lambda})$ is a measure of the buckling load. Equation (54) is solved by a similar scheme, discussed in Sec. IV. The matrix $[P]$ is symmetric in nature. The results have been presented in the following sections.

VI. Results

In this section, initially, the results of the mathematical model, which is developed to study the effects of bridging (Sec. V), are

Table 1 Comparison of normalized buckling loads of a present mathematical model and Simitses et al. [3] for a homogeneous clamped beam with a single delamination

b/L	$H_6 = 0.1H$		$H_6 = 0.3H$		$H_6 = 0.5H$	
	Present	Simitses et al. [3]	Present	Simitses et al. [3]	Present	Simitses et al. [3]
0.2	0.24952	0.2495	0.99242	0.9924	0.99562	0.9956
0.4	0.06244	0.0624	0.53143	0.5314	0.84815	0.8481
0.6	0.02783	0.0278	0.24351	0.2435	0.54115	0.5411
0.8	0.01564	0.0156	0.13904	0.1390	0.35146	0.3514

compared with the available data in the literature for the homogeneous nonbridged delaminated beam case as the present type of problem is studied for the first time. Later, the effects of the lengths and locations (along thicknesswise and spanwise) of the delaminations (delaminations I and II) on the lower and upper bounds of the buckling load as well as the effects of bridging on the delamination buckling are presented. Selected results are presented as it is rather difficult to present all the possible combinations of the various parameters.

A. Homogeneous Bridged Beam with two Separated Delaminations

The accuracy of the mathematical model developed in Sec. V is verified by comparing the results of the homogeneous delaminated beam for clamped boundary conditions with Simitses et al. [3]. The length of delamination I (a/L) is shrunk to 0.001 and is kept at $d_1 = 0.45L$ and $H_2 = 0.01H$ to model it as a single delamination case, by always ensuring that the developed systematic homogeneous equations are valid in the entire analysis. The effective-bridging modulus in the mathematical model is set to a nominal value (i.e., 10^{-6}) to neglect the bridging and to model it as a delaminated beam without bridging. There is excellent agreement between the present results and that of Simitses et al. [3] observed for various lengths and locations of delamination II as shown in Table 1.

1. Influence of Lengths and Locations of Two Separated Delaminations on Lower and Upper Bounds of Buckling Loads

Figure 5 shows the effect of delamination II on the lower and upper bounds of the nondimensionalized buckling loads ($\bar{P}$) for various locations of delaminations I and II ($H_2 = H_6 = 0.1H$, $0.2H$, and $0.3H$, respectively). The length of delamination I is $0.1L$ and $d_1 = 0.425L$. $\bar{P}(=P/P_{cr})$ is the ratio of the buckling load of the bridged trilayer beam with two separated delaminations and the buckling load of an intact (no delamination) trilayer beam of the same size. As the length of delamination II increases, the upper and lower bounds of the buckling load decrease, for given locations of delaminations I and II. In the case of the lower bounds of the buckling load, a local buckling mode occurs as the length of delamination II increases beyond $0.2L$, $0.4L$, and $0.5L$, respectively [30].

Whereas for the case of the upper bounds of the buckling load, a mixed buckling mode occurs, once $b/L > 0.25$. The gap between the upper and lower bounds of the buckling loads is higher for thin and longer delaminations, that is, $H_2 = H_6 = 0.1H$ and $b/L > 0.2$ (when $a/L = 0.1$). This suggests that the bridging could be effective for thin delaminations than for the deep delaminations ($H_2 = H_6 = 0.3H$). When the length of delamination I is increased to $0.5L$, the effects of delamination II on the lower and upper bounds of the buckling load are shown in Fig. 6. The variation in the lower bounds of the buckling load is nominal for the thin delamination case, that is, when $H_2 = H_6 = 0.1H$. Whereas when the two separated delaminations are located at $H_2 = H_6 = 0.2H$, when $b/L > 0.3L$ the lower bounds of the buckling loads decrease rapidly. In the case of the upper bounds of the buckling load, a monotonic relation between the length of delamination II and the buckling load is observed. Figure 7 shows the effects of delamination II and delamination I on $\bar{P}$ when the delaminations are located at $H_2 = 0.2H = H_6$. In the case of the lower bounds of the buckling load, the curves of $a/L = 0.1$ and $a/L = 0.3$ merge into a single line when $b/L > 0.35$. From this behavior we noted that the longer delamination (a/L or b/L) of the two separated delaminations influences the buckling load more than that of the shorter delamination. In the case of the upper bounds of the buckling load, the buckling load decreases gradually as the length of delamination II increases further. It is interesting to note that in the case of the upper bounds of the buckling load, the load distribution is proportional to individual subbeam's flexural rigidities as subbeams 2 and 3 deflect together [as given in Eq. (9)]. Whereas for the cases of the lower bounds, the load distribution is proportional to an individual subbeam's axial stiffnesses as subbeams 2 and 3 deflect independently and a possible local, global, and/or mixed

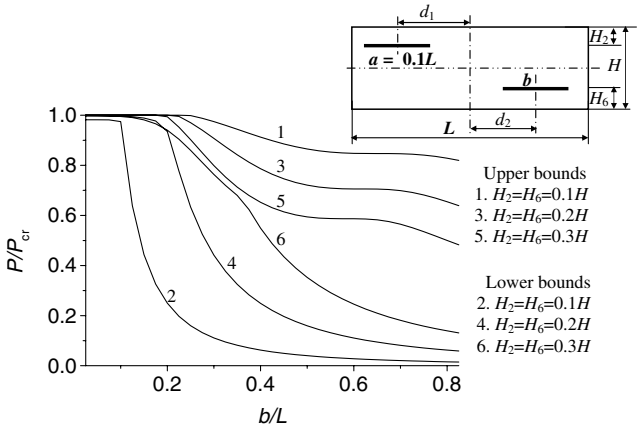

Fig. 5 Effects of delaminations I and II on the lower and upper bounds of the nondimensionalized buckling loads, $a = 0.1L$.

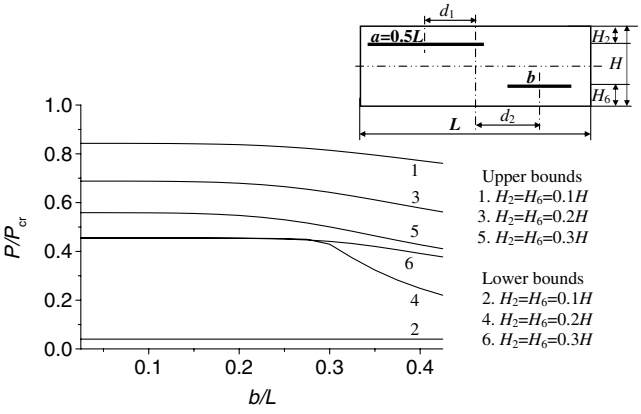

Fig. 6 Effects of delaminations I and II on the lower and upper bounds of the nondimensionalized buckling loads, $a = 0.5L$.

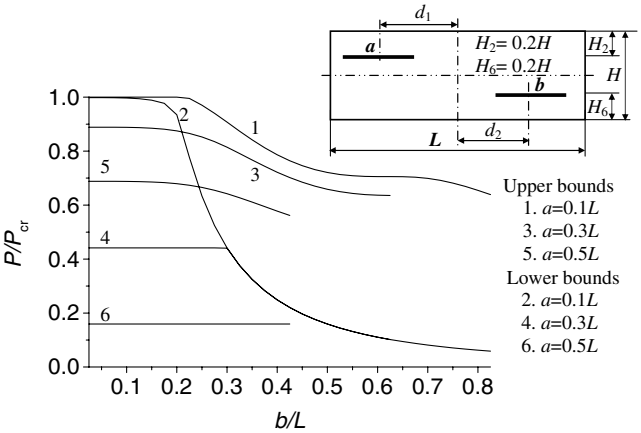

Fig. 7 Effects of delaminations I and II on the lower and upper bounds of the nondimensionalized buckling loads, $H_2 = H_6 = 0.2H$.

delamination buckling occurs [3,28,33]. In this case of the lower bounds of the buckling load, before buckling occurs, the axial strains in subbeams 2 and 3 are identical. When buckling takes place, the axial stress in the buckled subbeam decreases. This induces changes in the axial forces in subbeams 2 and 3.

After obtaining an overview of the lower and upper bounds of the buckling load for various locations and sizes of the separated delaminations, the effects of bridging on the buckling load are studied in the following section.

2. *Influence of Bridging on Buckling Loads*

Figure 8 shows the effect of bridging (in terms of the effective-bridging modulus, BM) on the nondimensionalized buckling load ($\bar{P}$) for various lengths of delamination II (b) when the length of delamination I is $a = 0.1L$, $d_1 = 0.425L$, $d_2 = 0.475L - b$, and $H_2 = H_6 = 0.1H$. When BM is very low (BM ≤ 0.0001), the buckling load values approach that of the lower bounds and the same trend continues thereafter. When BM is high (BM $= 10.0$), for shorter lengths of delamination II ($b < 0.4L$), the buckling load values approach that of the upper bounds. As the length of delamination II increases further the buckling loads decrease rapidly. As the BM increases, the buckling load increases and is bounded by the upper and lower bounds of the buckling load. A small variation in BM causes a large variation in the buckling load which shows the strong influence of bridging on the delamination buckling. We observed a monotonic relation between BM and $\bar{P}$. Similar observations were noted by the current authors [28] for a case of a two-layer delaminated beam with bridging and by Hu et al. [20], for a case of bridged beams with a circular delamination. Figure 9 shows the effect of bridging on $\bar{P}$ for various lengths of delamination II (b) when the length of delamination I is $a = 0.3L$, $d_1 = 0.325L$, $d_2 = 0.475L - b$, and $H_2 = H_6 = 0.1H$. From Fig. 9 it is observed that the variation of the buckling load is divided into two regions. In region I, the effect of bridging is nominal for shorter lengths of delamination II ($b/L < 0.4$). As the length of delamination II increases further, the buckling load decreases rapidly. It is observed that for the case of the thin film delaminations (when the thickness of the subbeams is less than $0.1H$) of moderate lengths (delaminations I and II), the bridging is found to be effective. Figure 10 shows the effect of BM on $\bar{P}$ for various lengths of delamination II when delaminations I and II are located at thicknesswise positions of $H_2 = H_6 = 0.2H$. The length of delamination I is $0.3L$ and $d_1 = 0.325L$. From Fig. 10 it is observed that as delamination II moves toward the center of the beam (deep delamination), the upper bounds of the buckling load decrease and at the same time, the lower bounds of the buckling load increase. Depending upon the lengths of delaminations I and II, the effect of the bridging on the buckling load decreases rapidly and a similar trend to that of the lower bounds follows. Further we noted that for longer and deep delaminations the influence of the bridging on the buckling load fades away and all the curves merge into a single line. For shallow delaminations ($H_6 \geq 0.2H$ and $H_2 = 0.1H$) of moderate lengths ($b = 0.35L$ to $0.50L$ and $a/L = 0.3$), the bridging is found be effective. This observation will vary based on the lengths of delamination I. We also observed that the thicknesses of the individual subbeams play a vital role in influencing the buckling load besides the delamination lengths. For the case of the deeply located delaminations, if the thickness of subbeam 8 reduces to less than $0.1H$ then local buckling occurs [30]. Therefore, an optimal level of bridging should be sought to maximize the compressive load bearing capability of a trilayer delaminated beam.

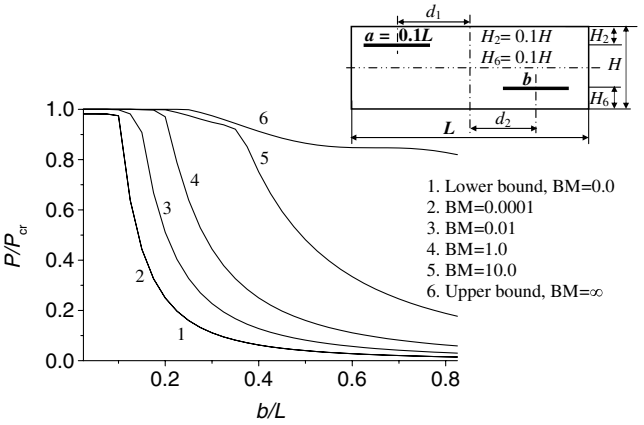

Fig. 8 Effects of bridging on the nondimensionalized buckling loads, $H_2 = H_6 = 0.1H$ and $a = 0.1L$.

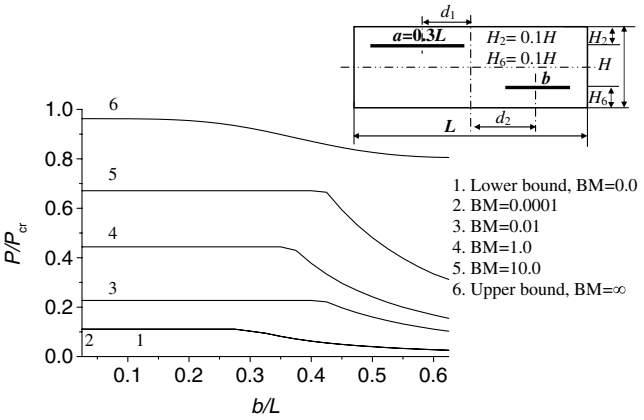

Fig. 9 Effects of bridging on the nondimensionalized buckling loads, $H_2 = H_6 = 0.1H$ and $a = 0.3L$.

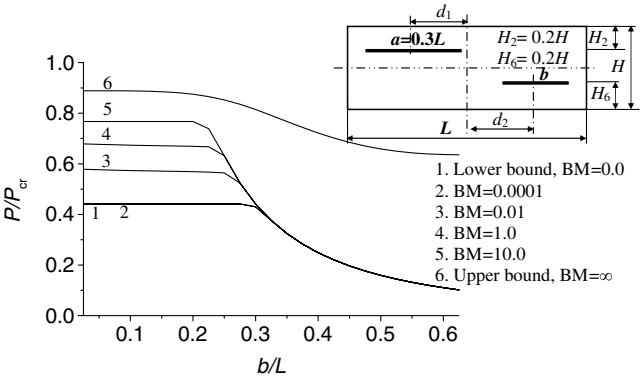

Fig. 10 Effects of bridging on the nondimensionalized buckling loads, $H_2 = 0.2H$, $H_6 = 0.2H$, and $a = 0.3L$.

3. *Influence of Spanwise Positions of Delamination II on Lower and Upper bounds of Buckling Loads*

Figure 11 shows the influence of the spanwise position of delamination II (d_2/L) on the lower and upper bounds of the nondimensionalized buckling load for various lengths of delaminations I and II and $H_2 = 0.1H = H_6$. Delamination I is located at $d_1 = 0.3375L$. Based on the lengths of delaminations I and II, the spanwise position of delamination II is restricted as shown in Fig. 11 and the curves end abruptly. The spanwise position of delamination II is zero, that is, $d_2/L = 0.0$ means that delamination II is located at the center of the beam as shown at the bottom of Fig. 11. From Fig. 11, it is observed that the spanwise position of delamination II has a strong influence on the upper bounds of the buckling loads. Whereas a notable effect on the lower bounds of the buckling load is observed when delamination II is located deep inside, that is, $H_2 = H_6 = 0.4H$ as shown in Fig. 12. For thin delamination cases ($H_2 = 0.1H = H_6$), from Fig. 11, it is observed that for longer delaminations ($a = 0.3L$, $b = 0.4L$), the upper bounds of the buckling load are maximum when delamination II is located at the center of the beam and the upper bounds reduce as delamination II moves away from the center of the

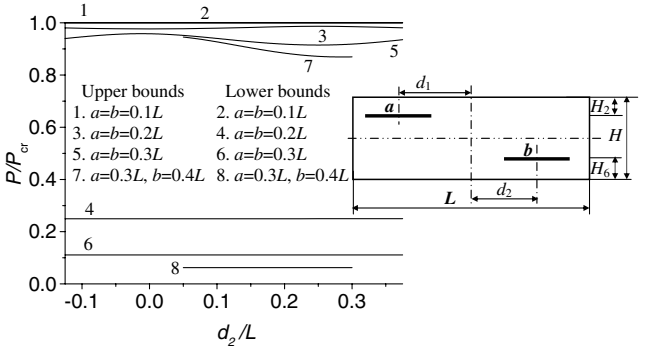

Fig. 11 Effects of the spanwise positions of delamination II on the lower and upper bounds of the nondimensionalized buckling loads, $H_2 = 0.1H = H_6$, $d_1 = 0.3375L$.

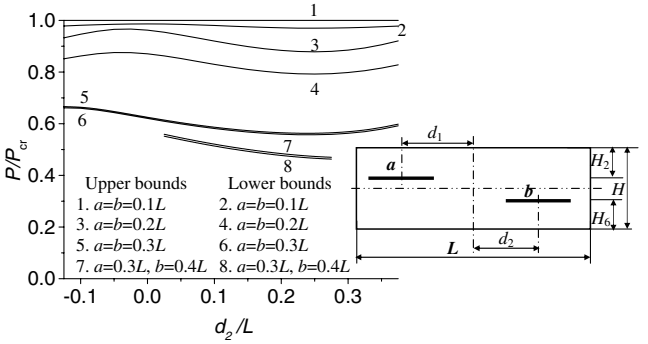

Fig. 12 Effects of the spanwise positions of delamination II on the lower and upper bounds of the nondimensionalized buckling loads, $H_2 = 0.4H = H_6$, $d_1 = 0.3375L$.

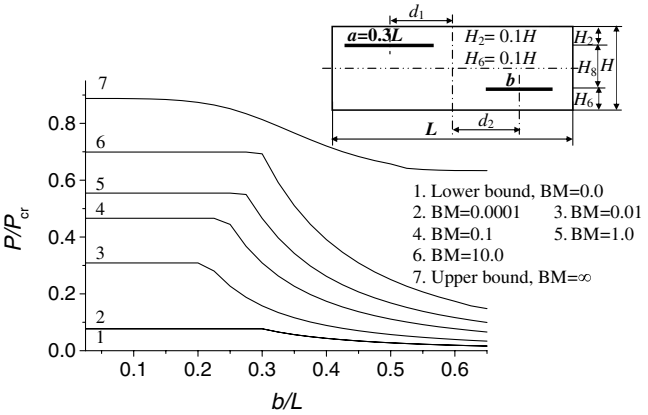

Fig. 13 Effects of bridging on P/P_{cr} of the trilayer beam ($H_2 = 0.1H =$ carbon/epoxy, $H_8 = 0.8H =$ glass/epoxy, and $H_6 = 0.1H =$ carbon/epoxy plies), $a = 0.3L$.

trilayer beam. When $a = b = 0.3L$, the upper bounds of the buckling load reach a maximum limit for $d_2 = 0.0$ and later the upper bounds reduce initially and increase further as delamination II moves away from the center of the trilayer beam. The lower bounds of the buckling load hardly depend on the spanwise positions of delamination II. As the delamination is deeply located as shown in Fig. 12 ($H_2 = 0.4H = H_6$), the lower bounds of the buckling load follow the similar trend as that of the upper bounds. Here, the upper bound values decrease when delamination II moves toward the end of the beam whereas the lower bound values increase. This suggests that the lower and upper bounds of the buckling load strongly depend on the spanwise as well as the thicknesswise positions of the two separated delaminations.

The following section deals with the parametric studies of the trilayer delaminated beam with bridging.

B. Trilayer Bridged Beam with Two Separated Delaminations

1. Influence of Bridging on Buckling Loads

The present mathematical model allows different material properties for a trilayer bridged beam with two separated delaminations. This enables one to study bridging effects on a wide range of trilayer beams with two separated delaminations. Figure 13 shows the effect of bridging on the buckling load of a trilayer delaminated beam. The trilayer beam is made of 0^0 plies of carbon/epoxy, glass/epoxy, and carbon/epoxy layers and the delaminations are located at the interface between the layers as shown in Fig. 13. $H_2 = 0.1H = H_6$ indicates the thickness of the carbon/epoxy layers and $H_8(H - H_2 - H_6)$ indicates the thickness of the glass/epoxy layers. The length of delamination I is $0.3L$, $d_1 = 0.425L$, and $H_2 = H_6 = 0.1H$. The material properties of glass/epoxy and carbon/epoxy plies are taken from the work of Hwang and Mao [34] which are given for glass/epoxy layers $E_x = 37.9$ GPa, $E_y = 14.3$ GPa, $G_{xy} = 5.6$ GPa, and $v_{xy} = 0.29$; and for carbon/epoxy layers $E_x = 121$ GPa, $E_y = 121$ GPa, $G_{xy} = 121$ GPa, and $v_{xy} = 0.23$. The upper and lower bounds of the buckling load are obtained based on the developed mathematical models, discussed in Secs. III and IV, respectively. From Fig. 13 we observed that the bridging strongly influences the buckling load. The bridging has a nominal effect on the buckling load when the delamination length is short, that is, $b/L < 0.3$ and when a/L is 0.3. But as the length of delamination II increases a strong influence of the bridging on the buckling load is observed. A small variation of BM has a strong influence on $\bar{P}$. The rapid variation in the buckling loads may be due to the change in the variation of buckling mode configurations. When the effective-bridging modulus is small (BM = 0.001) its influence is negligible. In that case, the buckling loads match that of a nonbridging delaminated beam case. As the effective-bridging modulus increases further (BM = 0.01), the buckling load bearing capability of a bridged beam increases which also depends on the length of delamination I. This indicates that a higher BM is essential for longer delaminations when the delaminated beam is thicker, that is, deeply located delaminations of longer length. Lower BM is sufficient to control the delamination buckling in the case of thinner delaminated beams if they contain short delamination, that is, shallow delaminations with short length. Hence, bridging has a strong influence on the delaminated beams based on the delamination locations and lengths. Though bridging increases the buckling loads, the stitch density may affect the structure's mechanical performance because damage (due to sewing operation) accumulates as stitches get closer. Therefore, an optimum level of stitching should be sought to maximize the strength and toughness of the trilayer beam.

2. Influence of Spanwise Position of Delamination II on Buckling Loads

Figure 14 show the influence of the spanwise position of delamination II (d_2/L) on the buckling load when $H_2 = 0.1H = H_6$

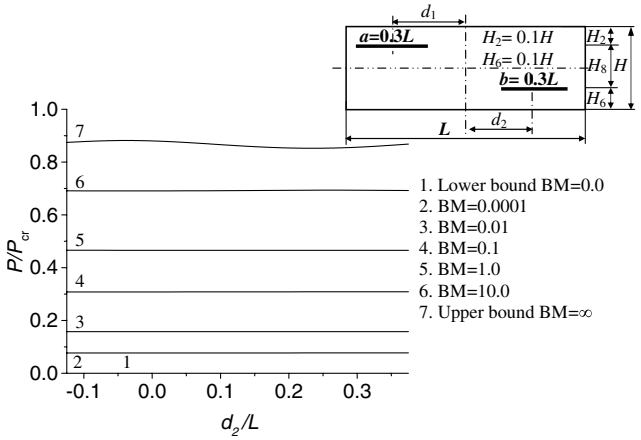

Fig. 14 Effects of the spanwise positions of delamination II on the nondimensionalized buckling loads of a trilayer beam, $H_2 = 0.1H = H_6$, $d_1 = 0.3375L$.

and $a = b = 0.3L$, for the trilayer beam configurations discussed in Fig. 13. Delamination I is located at an offset distance of $d_1 = 0.3375L$. The bridging has not affected the buckling loads when the spanwise positions of delamination II are varied. The upper bounds of the buckling loads are not influenced by the spanwise positions of delamination II.

VII. Conclusions

The buckling load of a trilayer bridged beam with two separated delaminations has been obtained by using an energy method and by solving it as an eigenvalue problem. The upper bounds of the buckling load have been accurately obtained by using the Euler–Bernoulli beam theory. A newly modified nondimensionalized parameter, effective-bridging modulus is introduced in the analysis to study the bridging effects on the buckling load. The BM is a function of the delamination length, slenderness ratio, and the relative bridging modulus, KL/E (where K is the bridging modulus and E is Young's modulus). The buckling load increases monotonically as the BM increases. The bridging improves the load bearing capability of a delaminated beam and an optimal level of stitching should be sought to maximize the compressive strength of laminate composites. It is worth noting that the longer of the two separated delaminations strongly influences the buckling load of the bridged beam. The bridging was found to be effective for the cases of thin and shallow delaminations of moderate lengths. Spanwise positions of separated delaminations strongly influence the upper bounds of the buckling load. The lower bounds and the buckling loads with bridging are effective for deeply located delaminations of longer lengths.

References

[1] Dransfield, K., Baillie, C., and Mai, Y. W., "Improving the Delamination Resistance of CFRP by Stitching—A Review," *Composites Science and Technology*, Vol. 50, 1994, pp. 305–317.

[2] Chai, H., Babcock, C. D., and Knauss, W. B., "One-Dimensional Modeling of Failure in Laminated Plates by Delamination Buckling," *International Journal of Solids and Structures*, Vol. 17, No. 11, 1981, pp. 1069–1083.

[3] Simitses, G. J., Sallam, S., and Yin, W. L., "Effect of Delamination of Axially Loaded Homogeneous Laminated Plates," *AIAA Journal*, Vol. 23, No. 9, 1985, pp. 1437–1444.

[4] Kardomateas, G. A., "Large Deformation Effects in the Postbuckling Behavior of Composites with Thin Delaminations," *AIAA Journal*, Vol. 27, No. 5, 1989, pp. 624–631.

[5] Chen, H. P., "Shear Deformation Theory for Compressive Delamination Buckling and Growth," *AIAA Journal*, Vol. 29, No. 5, 1991, pp. 813–819.

[6] Lee, J., Gurdal, Z., and Griffin, O. H., "Layer-Wise Approach for the Bifurcation Problem in Laminated Composites with Delaminations," *AIAA Journal*, Vol. 31, No. 2, 1993, pp. 331–338.

[7] Shu, D., and Mai, Y. W., "Buckling of Delaminated Composites Re-Examined," *Composite Science and Technology*, Vol. 47, No. 1, 1993, pp. 35–41.

[8] Gu, H., and Chattopadhyay, A., "A New Higher-Order Plate Theory in Delamination Buckling of Composite Laminates," *AIAA Journal*, Vol. 32, No. 4, 1994, pp. 1709–1716.

[9] Haiying, H., and Kardomateas, G. A., "Buckling of Orthotropic Beam-Plates with Multiple Central Delaminations," *International Journal of Solids and Structures*, Vol. 35, No. 13, 1998, pp. 1355–1362.

[10] Shu, D., "Buckling of Multiple Delaminated Beams," *International Journal of Solids and Structures*, Vol. 35, No. 13, 1998, pp. 1451–1465.

[11] Moradi, S., and Taheri, F., "Application of DQM as an Effect Solution Tool for Buckling Response of Delaminated Composite Plates," *Composite Structures*, Vol. 51, No. 4, 2001, pp. 439–449.

[12] Roberta, M., and Cox, B. N., "Concepts for Bridged Mode II Delamination Cracks," *Journal of the Mechanics and Physics of Solids*, Vol. 47, No. 66, 1999, pp. 1265–1300.

[13] Kim, J. K., Baillie, C. J. P., and Mai, Y. W., "Fracture Toughness of CFRP with Modified Epoxy Matrices," *Composites Science and Technology*, Vol. 43, No. 33, 1992, pp. 283–297.

[14] Kim, J. K., Mackay, D., and Mai, Y. W., "Drop-Weight Impact Tolerance of CFRP with Rubber Modified Epoxy Matrices," *Composites*, Vol. 24, No. 6, 1993, pp. 485–494.

[15] Hu, X. Z., and Mai, Y. W., "Mode-I Delamination and Fibre Bridging in Carbon Fibre/Epoxy Composites with and Without PVAL Coating," *Composites Science and Technology*, Vol. 46, No. 2, 1993, pp. 147–156.

[16] Shu, D., and Mai, Y. W., "Effect of Stitching on Interlaminar Delamination Extension in Composite Laminates," *Composites Science and Technology*, Vol. 49, No. 2, 1993, pp. 165–71.

[17] Shu, D., and Mai, Y. W., "Delamination Buckling with Bridging," *Composites Science and Technology*, Vol. 47, No. 1, 1993, pp. 25–33.

[18] Cox, B. N., "Delamination and Buckling in 3D Composites," *Journal of Composite Materials*, Vol. 28, No. 12, 1994, pp. 1114–1126.

[19] He, M., and Cox, B. N., "Crack Bridging by Through-Thickness Reinforcement in Delaminating Curved Structures," *Composites Part A: Applied Science and Manufacturing*, Vol. 29, No. 4, 1998, pp. 377–393.

[20] Hu, Y.-T., Huang, Y.-Y., Li, S.-P., and Zhong, W.-F., "The Effects of Bridging in a 3D Composite on Buckling, Postbuckling and Growth of Delamination," *Archive of Applied Mechanics*, Vol. 69, No. 6, 1999, pp. 419–428.

[21] Pan, T. S., and Herrington, P. D., "Local Buckling of Stitched Composite Laminate," *Composites: Part B*, Vol. 30, No. 8, 1999, pp. 833–840.

[22] Li, S., Nie, J., Qian, J., Huang, Y., and Hu, Y., "Initial Post-Buckling and Growth of a Circular Delamination Bridged by Nonlinear Fibers," *Journal of Applied Mechanics*, Vol. 67, No. 4, 2000, pp. 777–784.

[23] Gui, L., and Li, Z., "Delamination Buckling of Stitched Laminates," *Composites Science and Technology*, Vol. 61, No. 5, 2001, pp. 629–636.

[24] Daridon, L., and Zidani, K., "The Stabilizing Effects of Fiber Bridges on Delamination Cracks," *Composites Science and Technology*, Vol. 62, No. 11, 2002, pp. 83–90.

[25] Cartié, D. D. R., Cox, B. N., and Fleck, R., "Mechanism of Crack Bridging by Composite and Metallic Rods," *Composites Part A: Applied Science and Manufacturing*, Vol. 35, No. 11, 2004, pp. 1325–1336.

[26] Ivana, K. P., and Cartié, D. D. R., "Delamination Resistant Laminates by *Z*-Fiber® Pinning: Part I Manufacture and Fracture Performance," *Composites Part A: Applied Science and Manufacturing*, Vol. 36, No. 1, 2005, pp. 55–64.

[27] Freitas, G., Magee, C., Dardzinski, P., and Fusco, T., "Fiber Insertion Process for Improved Damage Tolerance in Aircraft Laminates," *International Journal of Advanced Materials*, Vol. 25, No. 4, 1994, pp. 36–43.

[28] Parlapalli, M., and Shu, D., "Buckling Analysis of Two-Layer Delaminated Beam with Bridging Effects," *European Journal of Mechanics-A/Solids* (to be published) doi:10.1016/j.euromechsol.2005.10.004.

[29] Shu, D., "Vibration of Sandwich Beams with Double Delaminations," *Composite Science and Technology*, Vol. 54, No. 1, 1995, pp. 101–109.

[30] Parlapalli, M., Dromaint, S., Shu, D., and Della, C. N., "Buckling Analysis of Three Layer Beams with Multiple Separated Delaminations," *Composite Structures*, Vol. 66, Nos. 1–4, 2004, pp. 53–60.

[31] Press, W. H., Saul, A. T., William, T. V., and Brain, P. F., *Numerical Recipes in FORTRAN: The Art of Scientific Computing*, Cambridge Univ. Press, New York, 1992, Chaps. 2 and 11.

[32] Lim, Y. B., and Parsons, I. D., "The Linearized Buckling Analysis of a Composite Beam with Multiple Delaminations," *International Journal of Solids Structures*, Vol. 30, No. 22, 1993, pp. 3085–3099.

[33] Parlapalli, M., and Shu, D., "Buckling of Two-Layer Beams with an Asymmetric Delamination," *Engineering Structures*, Vol. 26, No. 5, 2004, pp. 651–658.

[34] Hwang, S.-F., and Mao, C.-P., "The Delamination Buckling of Single-Fibre System and Interply Hybrid Composites," *Composite Structures*, Vol. 46, No. 3, 1999, pp. 279–287.

A. Roy
Associate Editor